Nonequilibrium axial charge production in expanding Glasma flux tubes

Naoto Tanji (ECT*)

arXiv:1805.00775

Gauge Topology 3: from Lattice to Colliders
June 1st 2018, ECT*

Outline

- Introduction
  - Chiral Magnetic Effect
  - Axial charge production in the early stage of heavy-ion collisions
- Formulation
  - Real-time lattice simulations
  - Color Glass Condensate initial conditions
  - Chiral anomaly and the Wilson fermion
- Numerical results
  - Uniform system
  - Flux tube configuration
- Summary

Chiral Magnetic Effect

Induction of electric current along a magnetic field in the presence of chirality imbalance

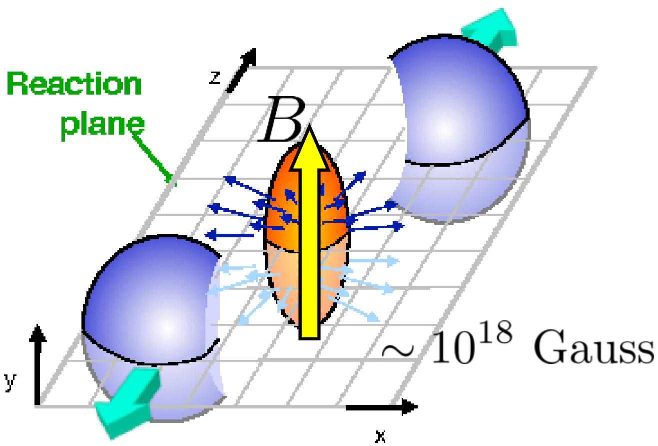

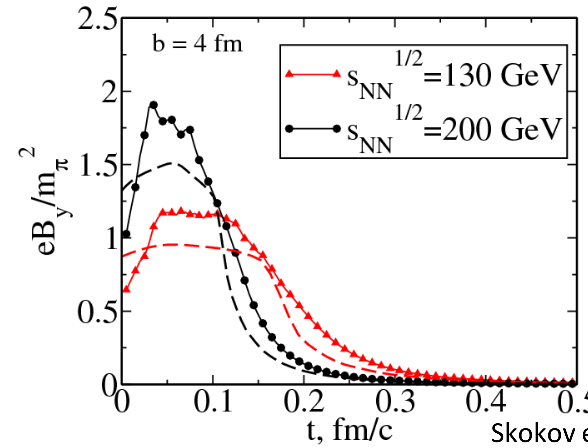

Skokov et al. (2009)

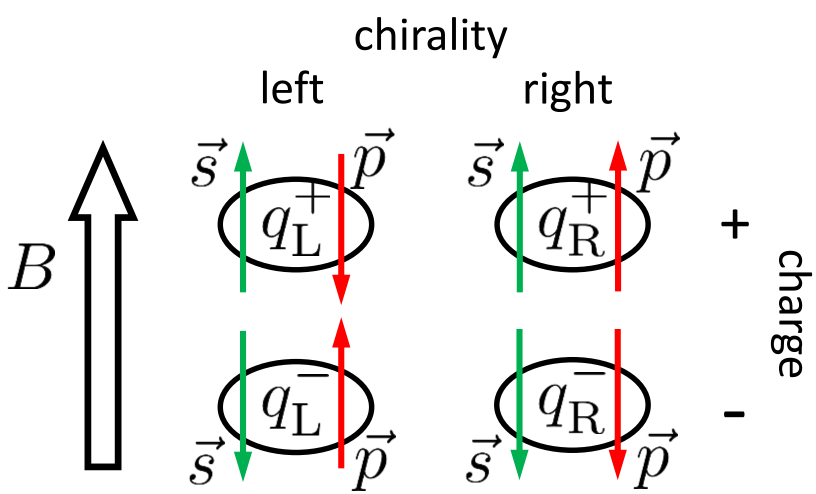

Chiral Magnetic Effect

Induction of electric current along a magnetic field in the presence of chirality imbalance

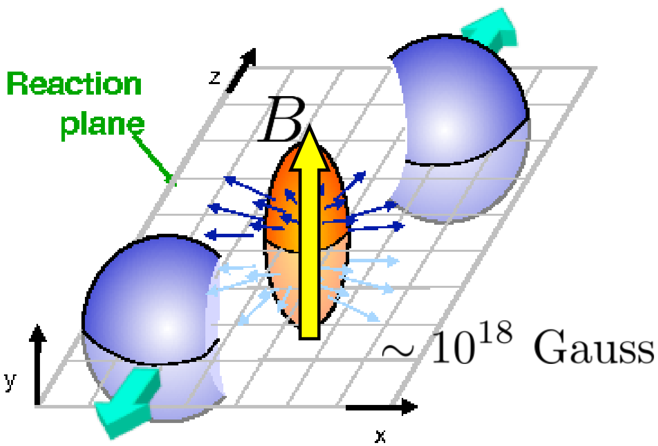

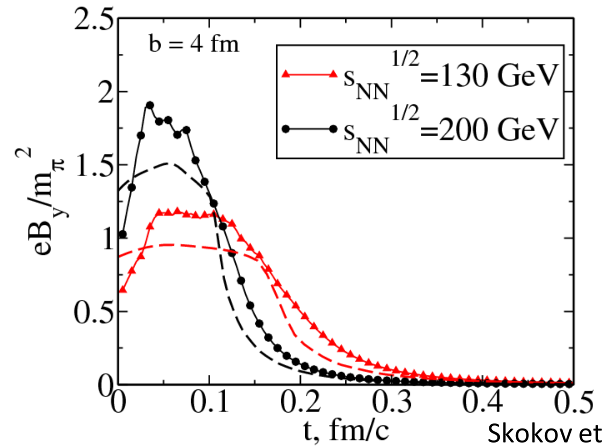

Skokov et al. (2009)

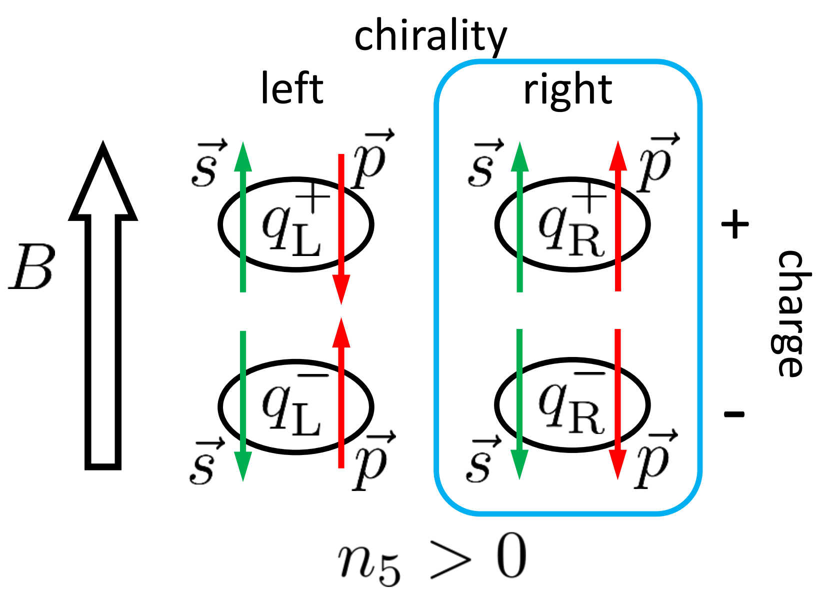

chirality imbalance

$$n_5 = \langle \psi^\dagger \gamma_5 \psi \rangle = \langle \psi_R^\dagger \psi_R \rangle - \langle \psi_L^\dagger \psi_L \rangle \neq 0$$

or $\mu_5 \neq 0$

electric current $\vec{J} = \dfrac{e^2}{2\pi^2} \mu_5 \vec{B}$

charge separation

Axial charge production in Glasma

Possible origins of the chirality imbalance in heavy-ion collisions:

- **Quark production in Glasma**
- Sphaleron transition in QGP/Glasma

Moore, Tassler (2011)
Mace, Schlichting, Venugopalan (2016)

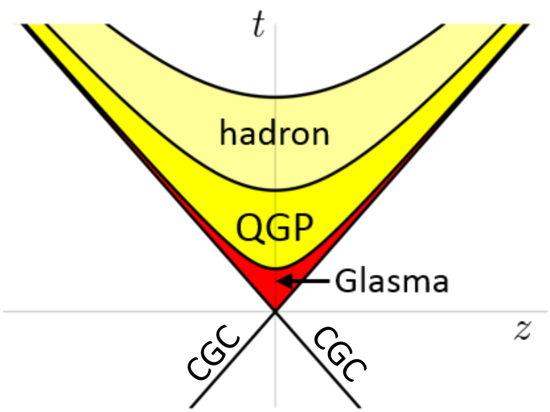

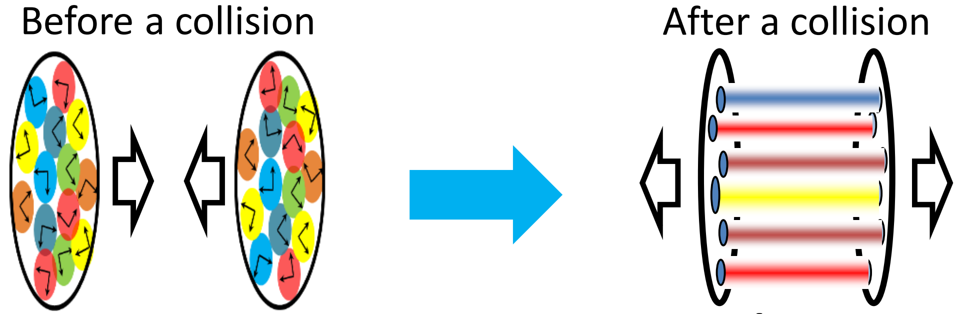

Color glass condensate (CGC)

$E_T^a \perp B_T^a$

Glasma

$E_L^a \parallel B_L^a$

$\boxed{F\tilde{F} \neq 0}$

Axial charge production in Glasma

Possible origins of the chirality imbalance in heavy-ion collisions:

- **Quark production in Glasma**
- Sphaleron transition in QGP/Glasma

Moore, Tassler (2011)
Mace, Schlichting, Venugopalan (2016)

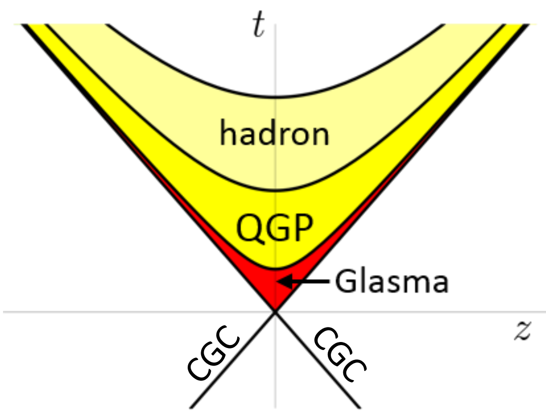

Before a collision | After a collision

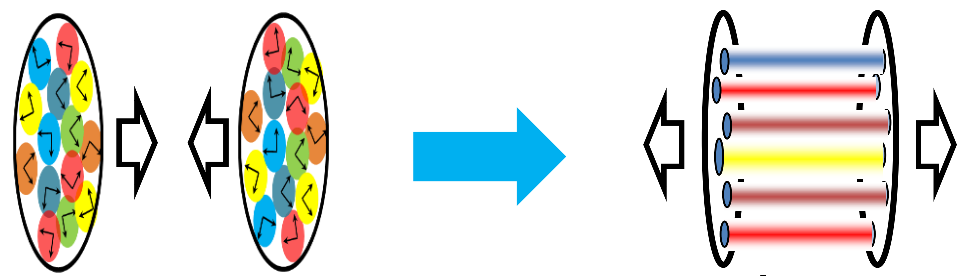

Color glass condensate (CGC)

$\boldsymbol{E}_T^a \perp \boldsymbol{B}_T^a$

Glasma

$\boldsymbol{E}_L^a \parallel \boldsymbol{B}_L^a$

$\boxed{F\tilde{F} \neq 0}$

Chromo E and B fields
U(1) B field
} exist only at the early stage.

→ All the processes are far-from-equilibrium.

Challenges:

Nonequilibrium, Nonperturbative, Quantum dynamics of quarks, Expanding geometry

Real-time lattice simulations of axial charge production

Real-time lattice simulations

Strong gauge fields $A \sim 1/g$ → classical approximation for the gauge fields

By systematic weak-coupling expansion around strong gauge fields, real-time evolution equations for classical(-statistical) gauge fields and dynamical quantum quark fields can be derived from the Schwinger-Keldysh path-integral formalism. Jeon (2014); Kasper, Hebenstreit, Berges (2014)

LO: Yang-Mills equations for boost-invariant classical gauge fields

$$[D_\mu, F^{\mu\nu}] = J^\nu$$

external current

Dirac equation for quark mode functions

$$[i\gamma^\mu(\partial_\mu + igA_\mu) - m]\,\psi_{\boldsymbol{p},s,c} = 0$$

- ➢ The backreaction from quarks to the gauge fields is negligible in the LO.
- ➢ These equations are solved with CGC initial conditions on the lattice in the expanding geometry.

$$\tau = \sqrt{t^2 - z^2}$$
$$\eta = \frac{1}{2}\ln\frac{t+z}{t-z}$$

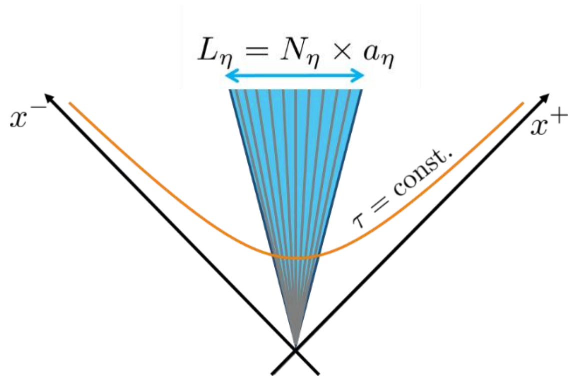

CGC initial conditions

Classical YM eqs. coupled to large-x color sources

$$[D_\mu, F^{\mu\nu}] = \delta^{\nu +}\delta(x^-)\rho_{(1)}(\boldsymbol{x}_\perp) + \delta^{\nu -}\delta(x^+)\rho_{(2)}(\boldsymbol{x}_\perp)$$

Solution at $\tau = 0^+$ in the Fock-Schwinger gauge $A^\tau = 0$

$$E_z(\tau = 0^+, \boldsymbol{x}_\perp) = -ig\left[\alpha^i_{(1)}, \alpha^i_{(2)}\right]$$

$$B_z(\tau = 0^+, \boldsymbol{x}_\perp) = -ig\epsilon^{ij}\left[\alpha^i_{(1)}, \alpha^j_{(2)}\right]$$

with

$$\alpha^i_{(n)}(\boldsymbol{x}_\perp) = \frac{i}{g}V^\dagger_{(n)}\partial_i V_{(n)}$$

$$V_{(n)}(\boldsymbol{x}_\perp) = \exp\left[-ig\nabla_\perp^{-2}\rho_{(n)}\right]$$

Kovner, McLerran, Weigert (1995)

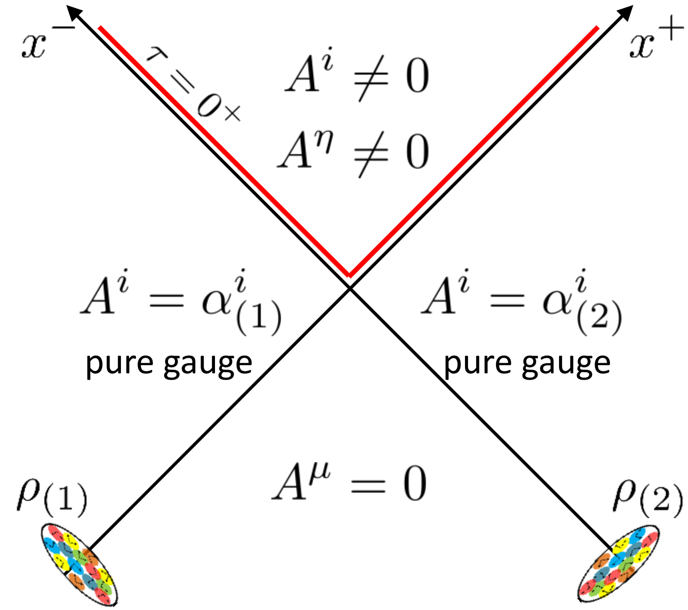

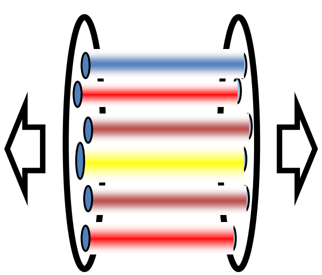

Glasma

$\boldsymbol{E}^a_L \parallel \boldsymbol{B}^a_L$

Numerical solution for $\tau > 0$ in the McLerran-Venugopalan (MV) model

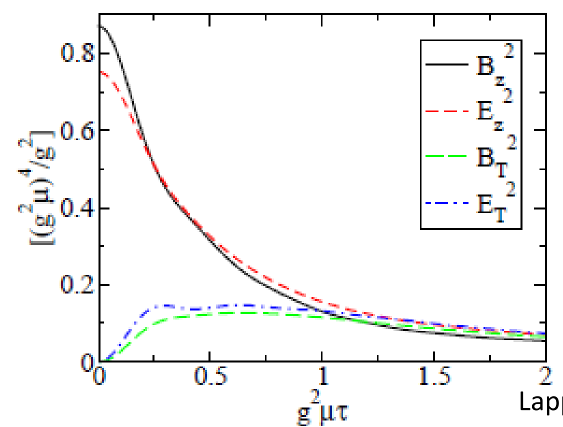

Lappi, McLerran (2006)

Glasma flux tube

Instead of random color distributions, we consider a fixed configuration that leads to single-flux-tube configuration of the SU(2) color fields with a Gaussian profile.

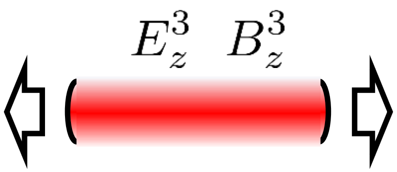

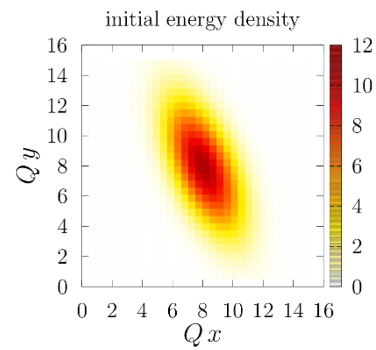

Remark 1: This is **not** a topological configuration.
Remark 2: Glasma flux tubes are **not** confining flux tubes.

Instead of random color distributions, we consider a fixed configuration that leads to single-flux-tube configuration of the SU(2) color fields with a Gaussian profile.

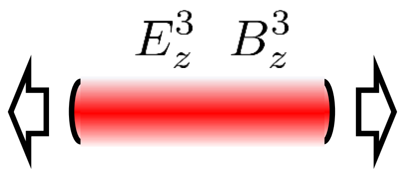

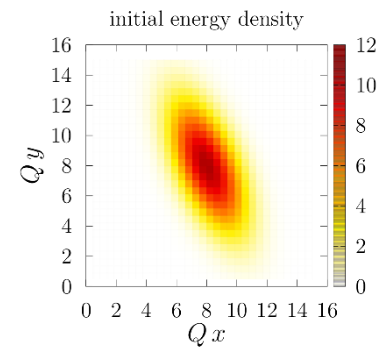

Remark 1: This is **not** a topological configuration.
Remark 2: Glasma flux tubes are **not** confining flux tubes.

Breaking of a confining flux tube

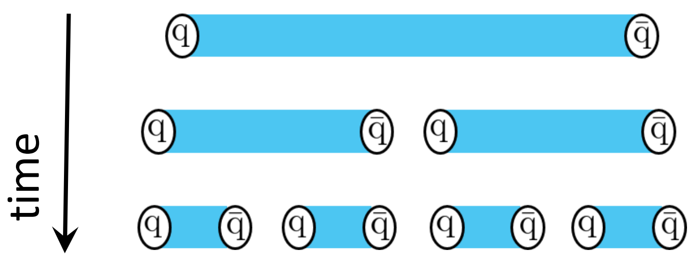

- Production of one pair immediately causes string breaking.

Decay of a Glasma flux tube

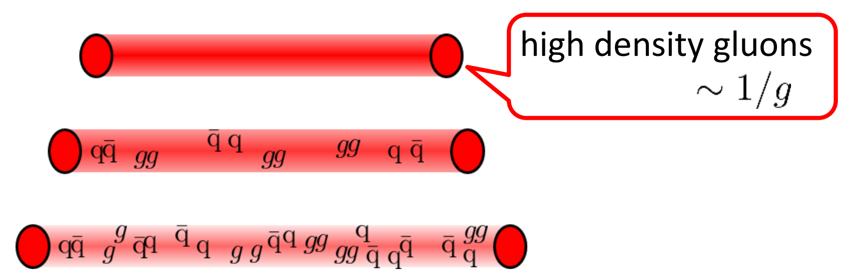

- Production of one pair is not enough to shield the field for weak coupling.
- The field is gradually diluted.

Quark fields

Up to the initial surface $\tau = 0^+$, the Dirac equation under the CGC classical gauge fields can be solved analytically.

Gelis, Kajantie, Lappi (2006);
Gelis, Tanji (2016)

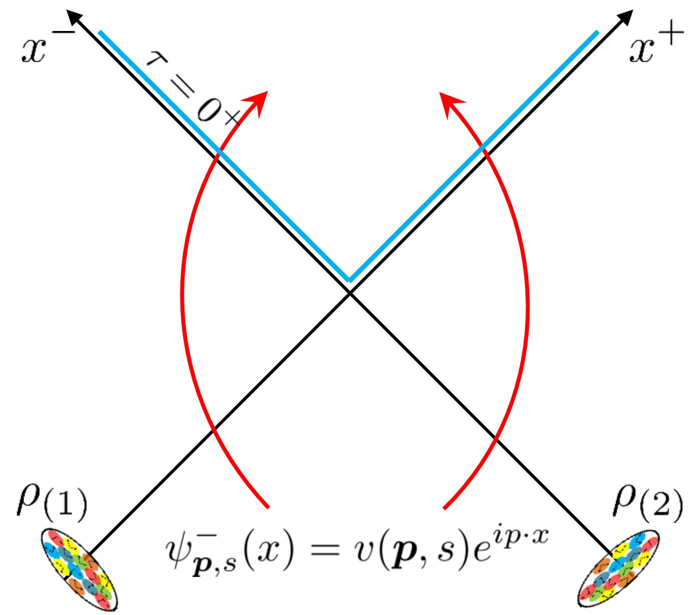

The evolution for $\tau > 0$ can be described by solving the Dirac equation for the mode functions

$$\left(i\gamma^0\partial_\tau + \frac{i}{\tau}\gamma^3 D_\eta + i\gamma^i D_i - m + W\right)\psi^-_{\boldsymbol{p}_\perp,\nu,s,c}(x) = 0$$

on the real-time lattice in the expanding geometry.

To realize the chiral anomaly on the lattice, we employ the Wilson fermion extended to the expanding geometry.

Tanji, Berges (2018)

Wilson fermion and chiral anomaly

Adler-Bell-Jackiw anomaly equation

$$\partial_\mu j_5^\mu = 2m\langle\overline{\psi} i\gamma_5\psi\rangle + \frac{g^2}{4\pi^2}\boldsymbol{E}^a\cdot\boldsymbol{B}^a$$

Axial current $j_5^\mu = \langle\overline{\psi}\gamma^\mu\gamma_5\psi\rangle$

The Wilson fermion exactly satisfies

$$\partial_\mu j_5^\mu = 2m\langle\overline{\psi} i\gamma_5\psi\rangle + \langle\overline{\psi} i\gamma_5 W\psi\rangle$$

where $W\psi$ is the Wilson term added to the Dirac equation to suppress doublers.

The axial anomaly is realized if

$$\langle\overline{\psi} i\gamma_5 W\psi\rangle \approx \frac{g^2}{4\pi^2}\boldsymbol{E}^a\cdot\boldsymbol{B}^a$$

which has been proven to hold in the continuum limit in the Euclidean lattice gauge theory,

Karsten, Smit (1981)

and numerically confirmed in real-time lattice computations for non-expanding systems.

Tanji, Mueller, Berges (2016);
Mueller, Hebenstreit, Berges (2016);
Mace, Mueller, Schlichting, Sharma (2017)

Anomaly equation in the expanding geometry

ABJ anomaly equation in the τ-η coordinates

$$\frac{1}{\tau}\partial_\tau\left(\tau j_5^\tau\right) + \partial_i j_5^i + \cancel{\frac{1}{\tau}\partial_\eta j_5^\eta} = \cancel{2m\langle\bar{\psi}i\gamma_5\psi\rangle} + \frac{g^2}{4\pi^2}\boldsymbol{E}^a\cdot\boldsymbol{B}^a$$

boost-invariant background $\qquad m \approx 0$

Axial charge density per unit transverse area and unit rapidity

$$\frac{dN_5}{d^2x_\perp d\eta} = \tau j_5^\tau(x)$$
$$= -\int_0^\tau \tau' \partial_i j_5^i \, d\tau' + \frac{g^2}{4\pi^2}\int_0^\tau \tau' \boldsymbol{E}^a\cdot\boldsymbol{B}^a \, d\tau'$$

Anomaly equation in the expanding geometry

ABJ anomaly equation in the τ-η coordinates

$$\frac{1}{\tau}\partial_\tau\left(\tau j_5^\tau\right) + \partial_i j_5^i + \cancel{\frac{1}{\tau}\partial_\eta j_5^\eta} = \cancel{2m\langle\bar{\psi} i\gamma_5\psi\rangle} + \frac{g^2}{4\pi^2}\boldsymbol{E}^a\cdot\boldsymbol{B}^a$$

boost-invariant background $\qquad m \approx 0$

Axial charge density per unit transverse area and unit rapidity

$$\frac{dN_5}{d^2x_\perp d\eta} = \tau j_5^\tau(x)$$

$$= -\int_0^\tau \tau' \partial_i j_5^i \, d\tau' + \frac{g^2}{4\pi^2}\int_0^\tau \tau' \boldsymbol{E}^a\cdot\boldsymbol{B}^a \, d\tau'$$

outflow in the transverse plane

source term

- In a uniform system or at very early times, the transverse divergence term is negligible. Then the axial charge density can be computed solely from the gauge fields.
- Otherwise, one needs to solve the Dirac equation.

Uniform Glasma

Take the limit of the flux tube width $\longrightarrow \infty$

Q : typical energy scale of the Glasma

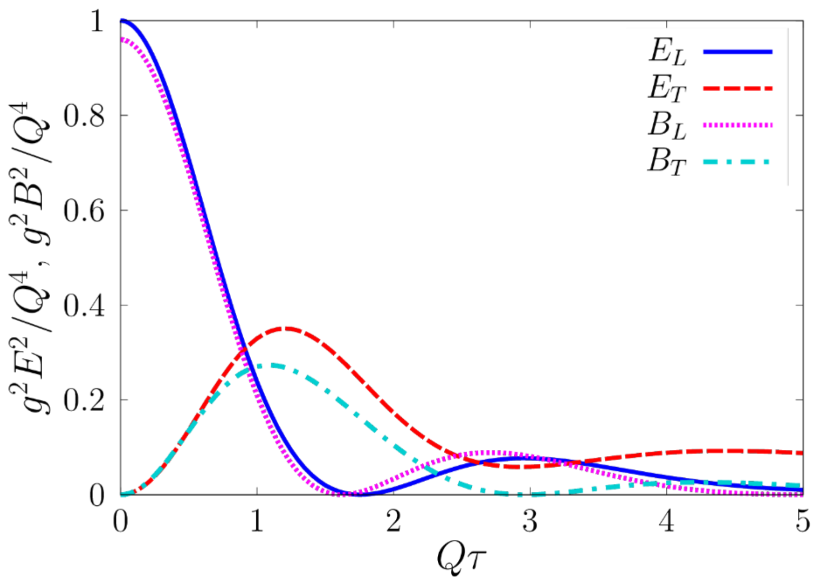

Time evolution of the field strength

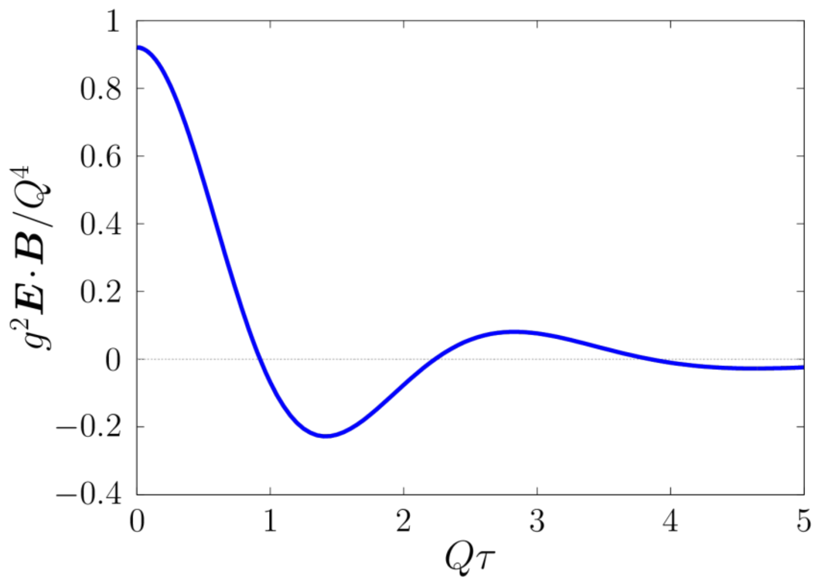

Time evolution of $\boldsymbol{E}\cdot\boldsymbol{B}$

- Similar behavior to that with the MV initial condition.
- In this uniform system, the decay of the fields is a purely nonlinear effect.

Uniform Glasma

$N_f = 1$
$m/Q = 0.01$
$N_x = N_y = 48,\ N_\eta = 512$

Verification of the anomaly relation

$$\frac{dN_5}{d^2x_\perp d\eta} \approx \frac{g^2}{4\pi^2}\int_0^\tau \tau' \boldsymbol{E}^a \cdot \boldsymbol{B}^a \, d\tau'$$

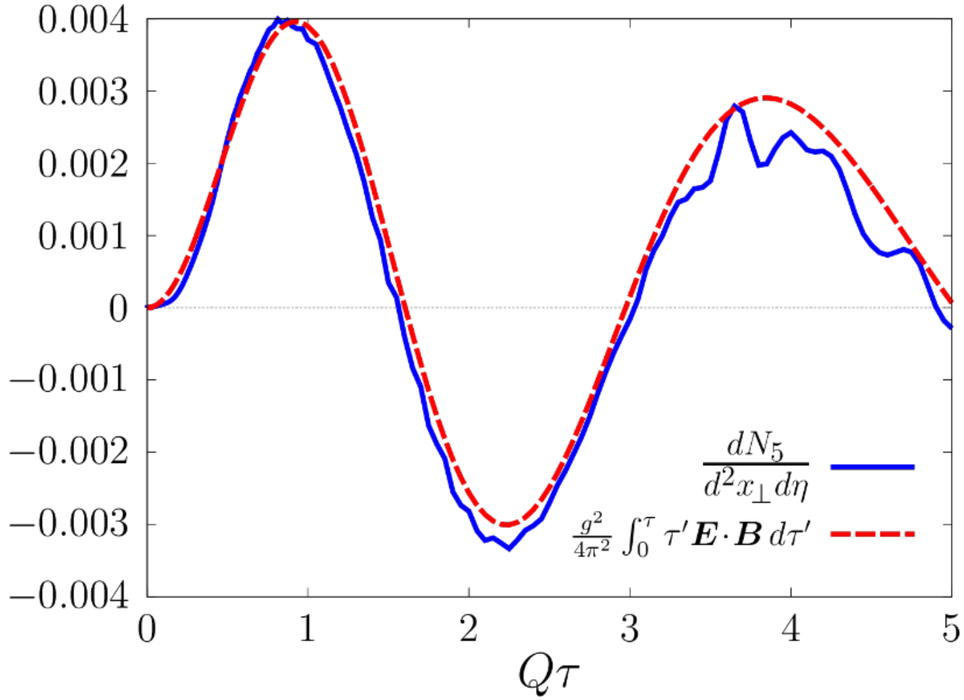

For $Q = 1\ \mathrm{GeV}$, $\frac{dN_5}{d^2x_\perp d\eta}/Q^2 = 0.004$ $\Longrightarrow$ 0.1 excess of right-quarks over left-quarks per flavor in a box with 1fm^2 transverse area and one unit of rapidity.

Quark mass dependence

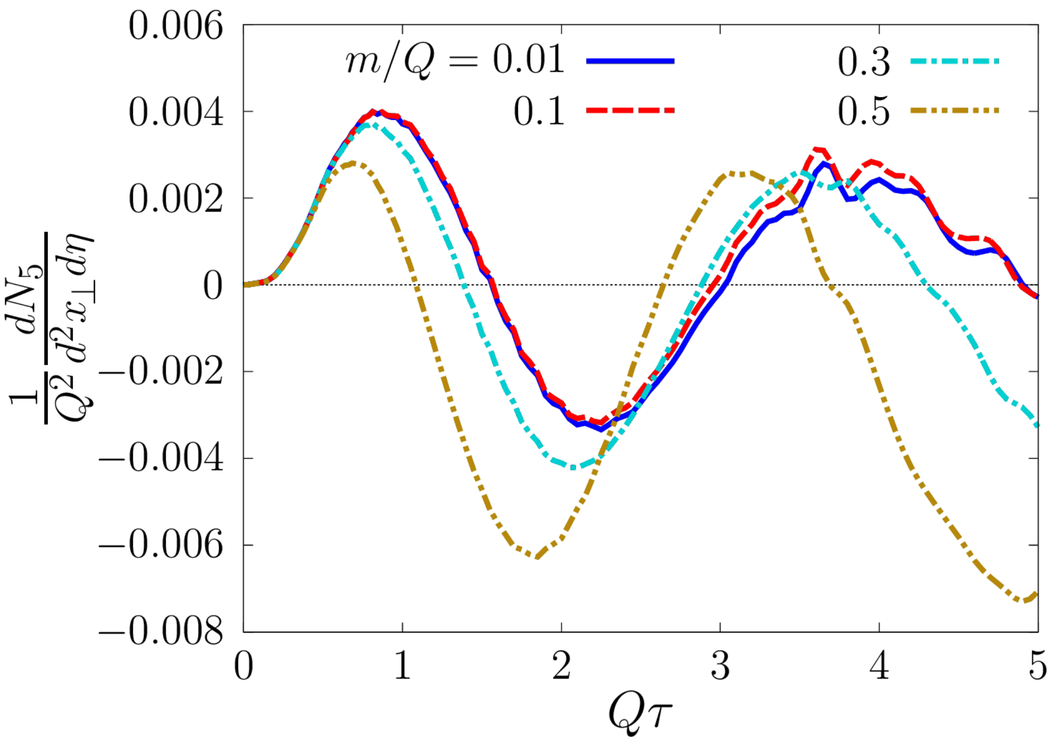

- Lighter quarks $m/Q \leq 0.1$ are almost degenerated.
- Heavier quarks are affected by the pseudo scalar condensate term.

$$\frac{dN_5}{d^2x_\perp d\eta} \approx 2m\int_0^\tau \tau' \langle \overline{\psi} i\gamma_5 \psi \rangle \, d\tau' + \frac{g^2}{4\pi^2}\int_0^\tau \tau' \boldsymbol{E}^a \cdot \boldsymbol{B}^a \, d\tau'$$

Effects of mass

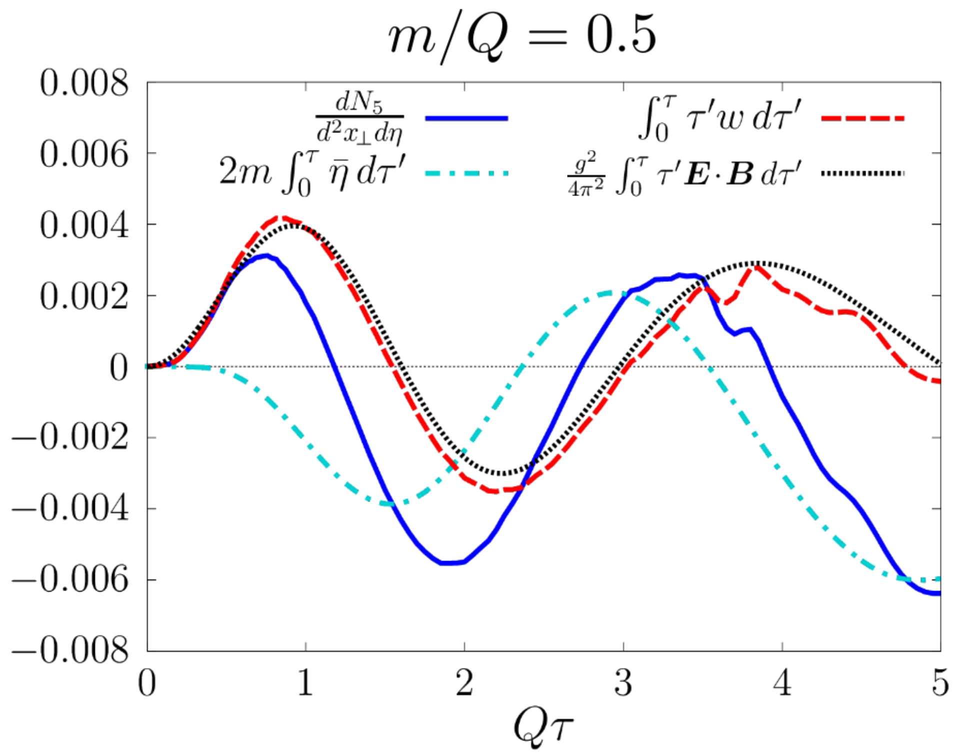

$$\frac{dN_5}{d^2x_\perp d\eta} \approx 2m\int_0^\tau \tau' \langle \overline{\psi} i\gamma_5 \psi \rangle \, d\tau' + \frac{g^2}{4\pi^2}\int_0^\tau \tau' \boldsymbol{E}^a \cdot \boldsymbol{B}^a \, d\tau'$$

- The pseudo scalar condensate term is comparable to other terms.
- The axial charge is not always diminished by the mass term.

Glasma flux tubes

The profile of flux tubes in the transverse plane

- Two flux tubes to satisfy the periodic b.c.
- Distorted Gaussian to have both E and B.

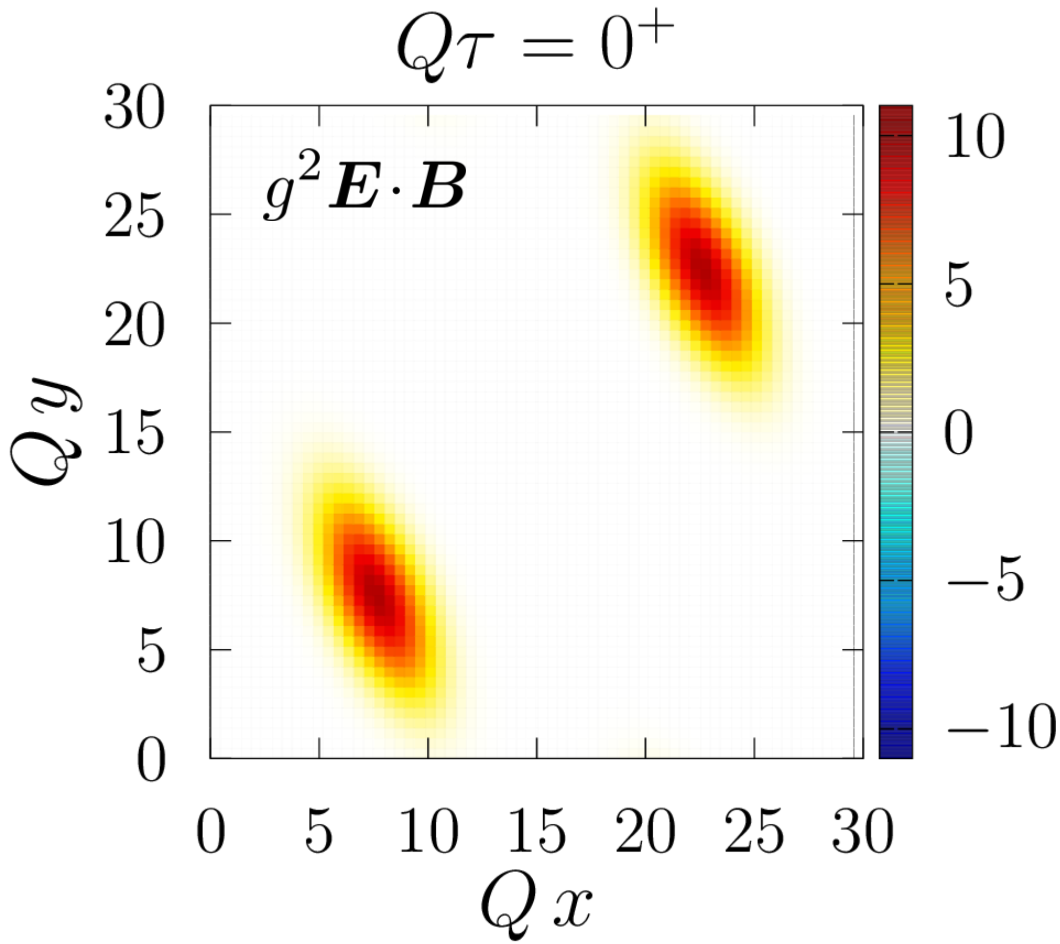

Glasma flux tubes

The profile of flux tubes in the transverse plane

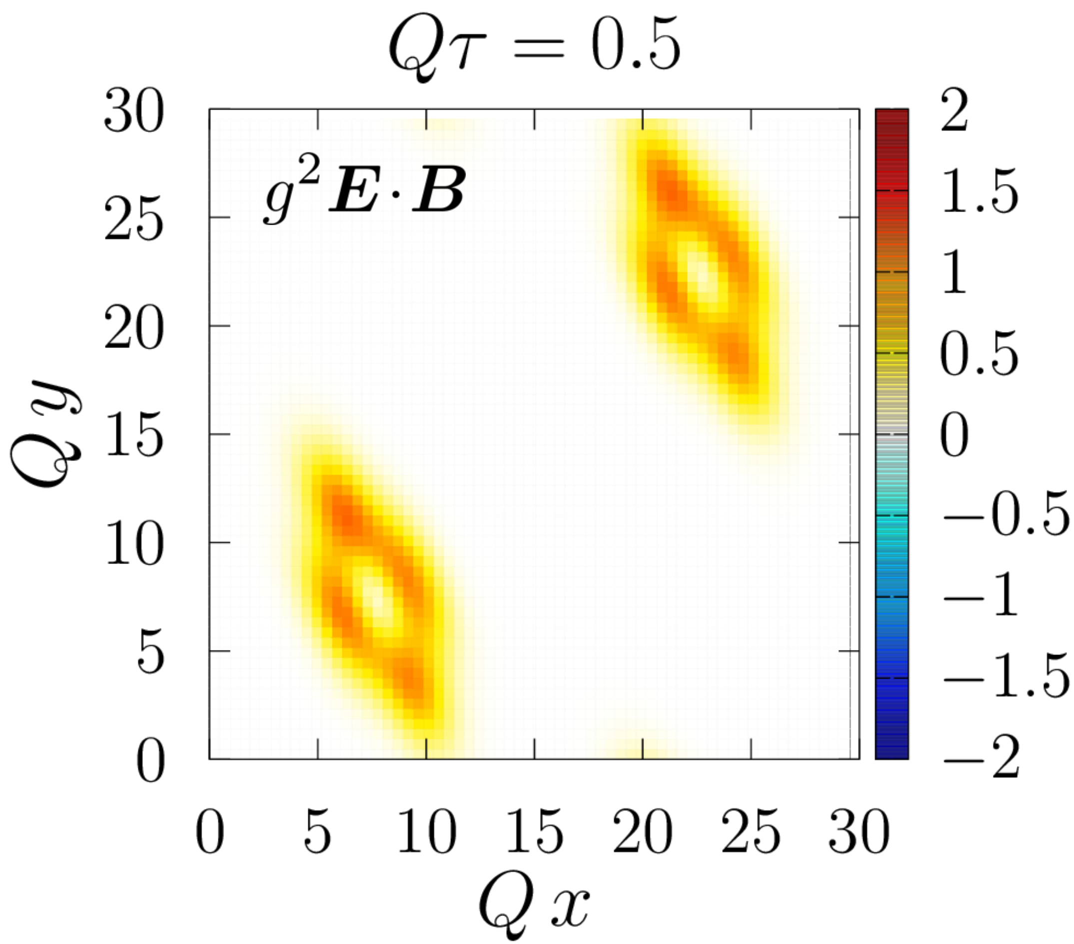

Glasma flux tubes

The profile of flux tubes in the transverse plane

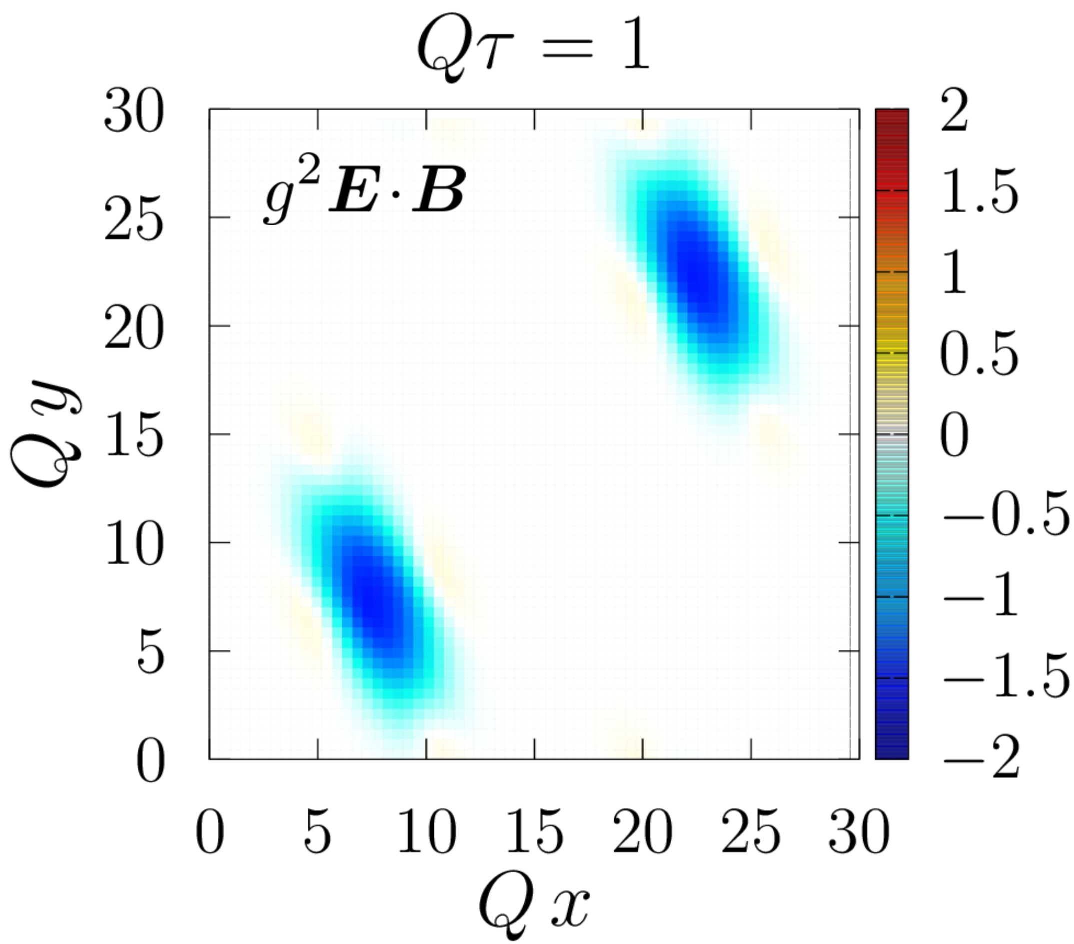

Glasma flux tubes

The profile of flux tubes in the transverse plane

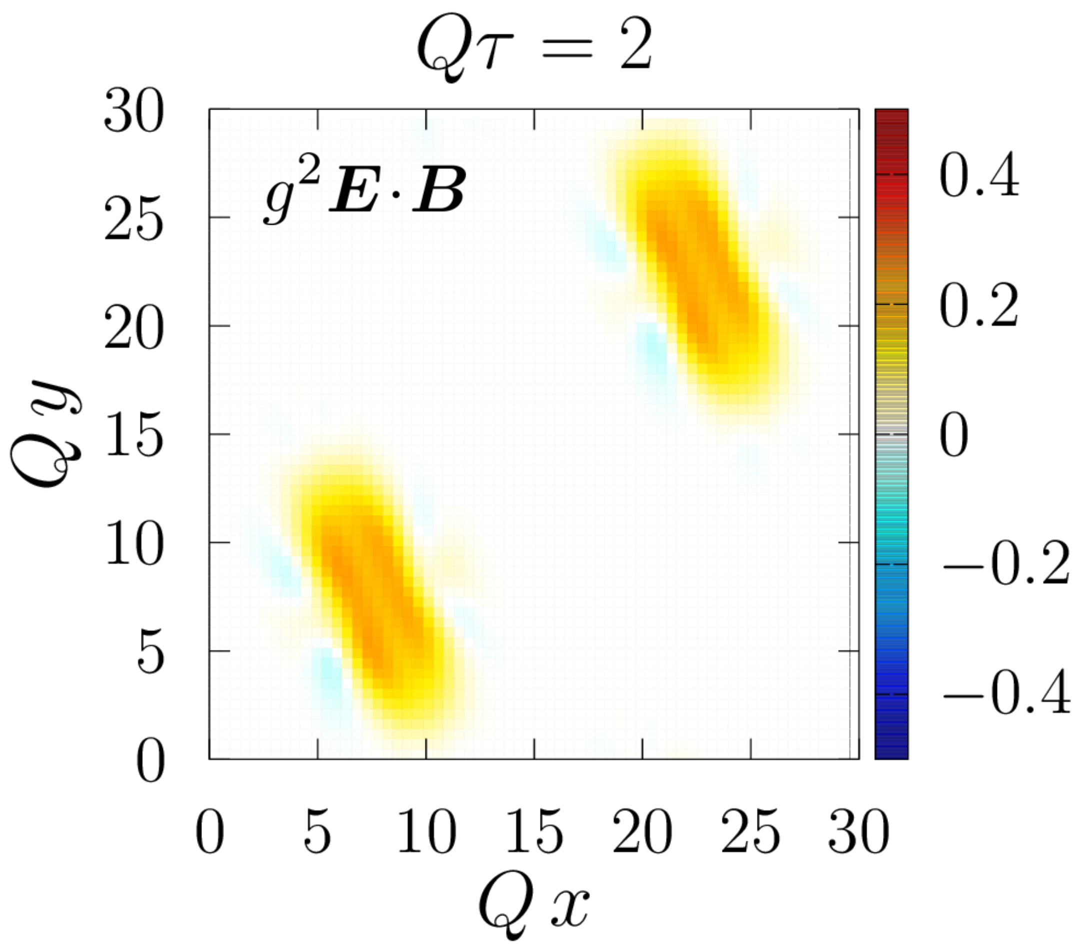

Glasma flux tubes

The profile of flux tubes in the transverse plane

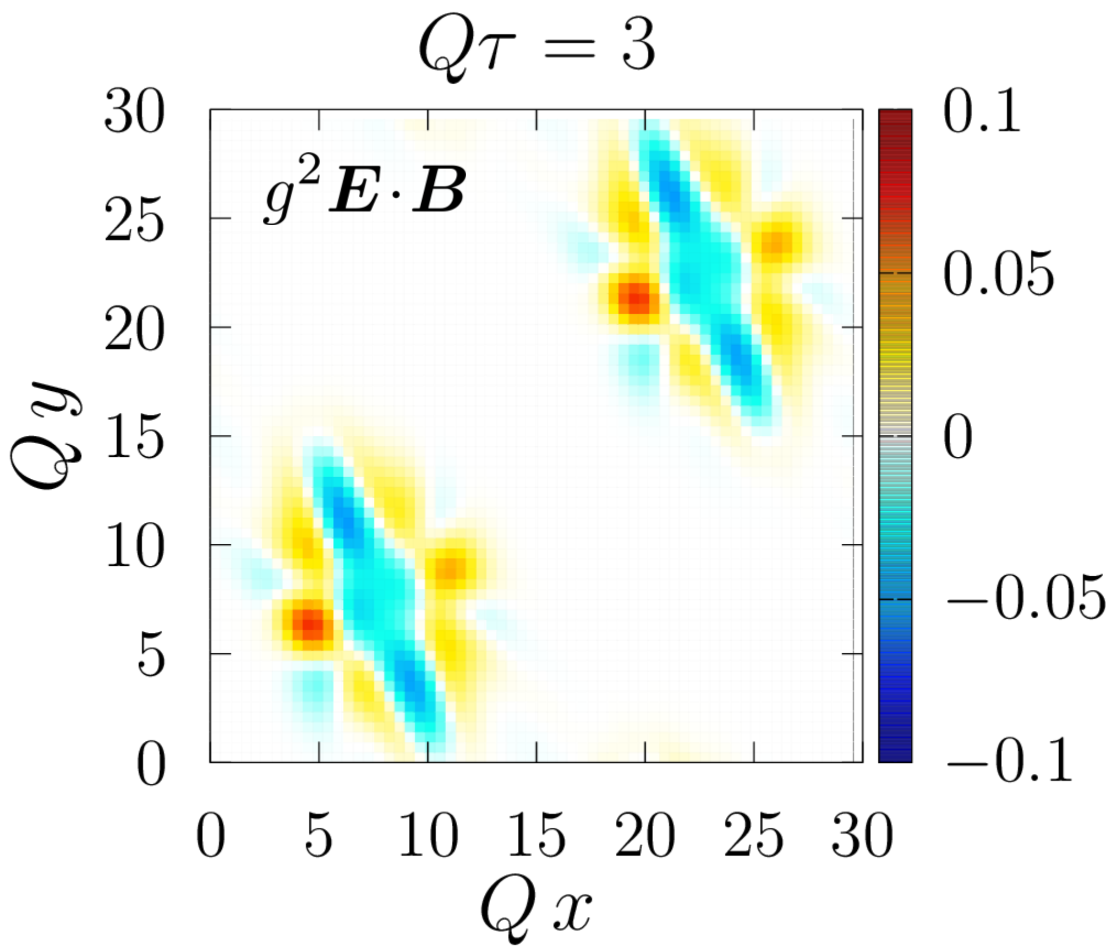

Glasma flux tubes

The profile of flux tubes in the transverse plane

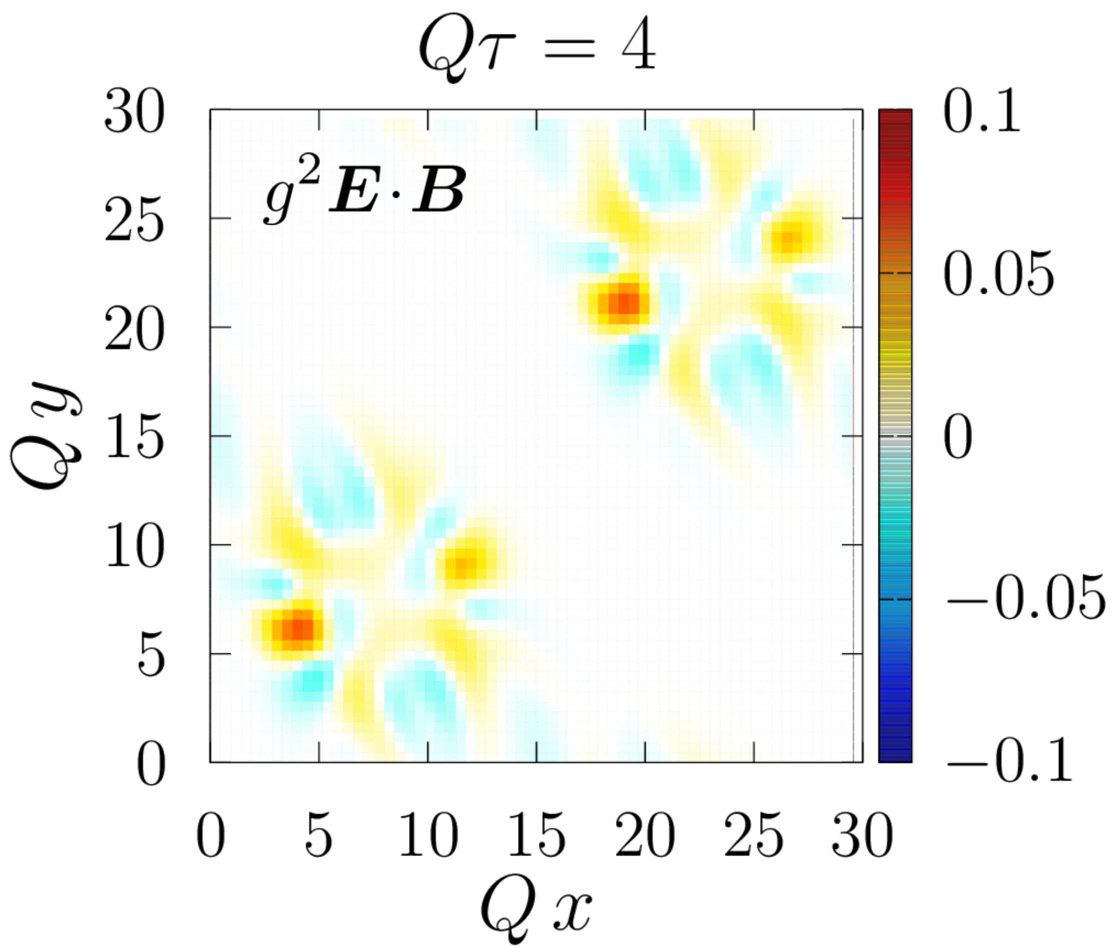

Glasma flux tubes

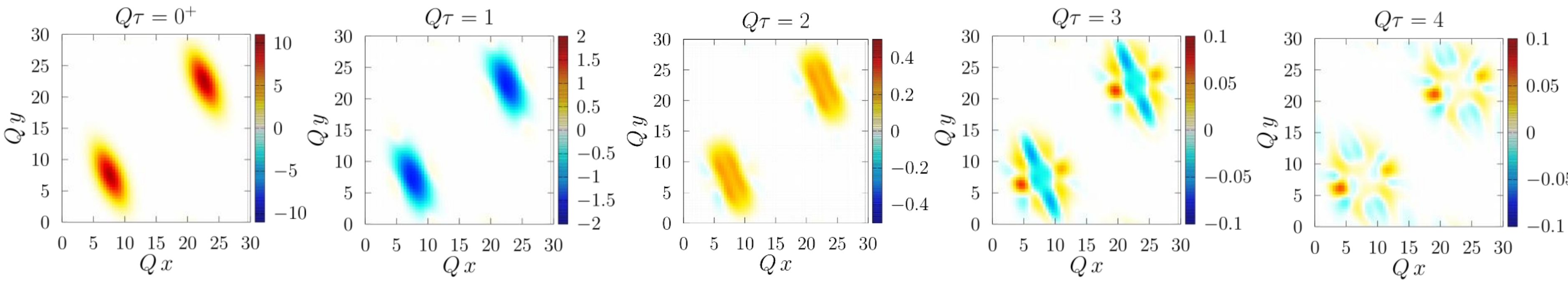

Transverse profiles of $\boldsymbol{E}\cdot\boldsymbol{B}$ for different times

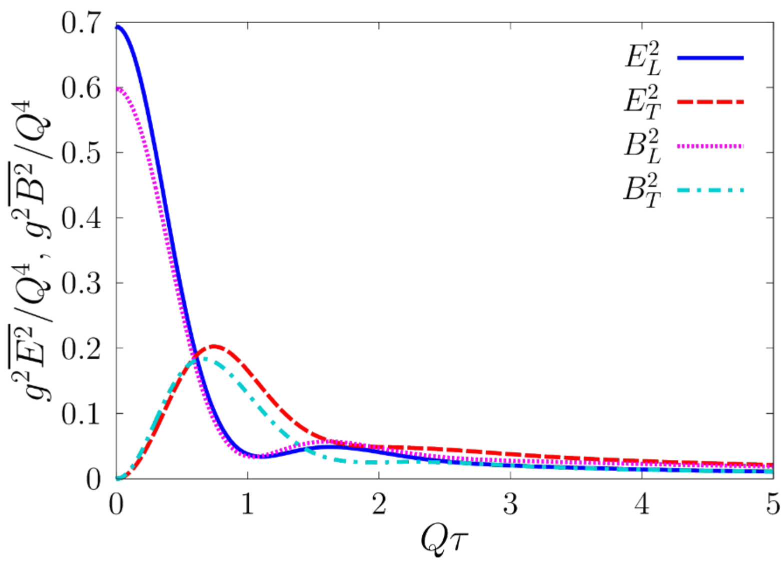

Time evolution of the space-averaged field strength

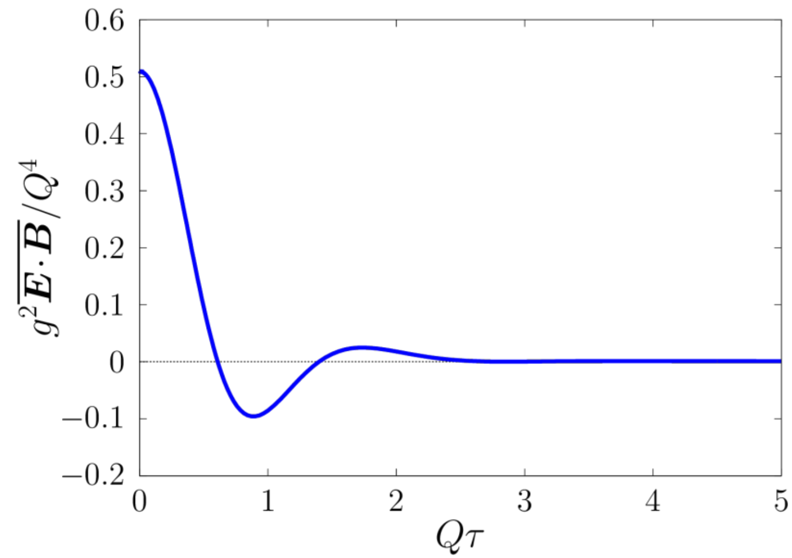

Time evolution of the space-averaged $\boldsymbol{E}\cdot\boldsymbol{B}$

- Similar behavior to that with the MV initial condition.
- The decay at later times is faster than the uniform case.

Glasma flux tubes

Verification of the space-averaged anomaly relation

$$\frac{\overline{dN_5}}{d^2x_\perp d\eta} \approx \frac{g^2}{4\pi^2}\int_0^\tau \tau' \overline{\boldsymbol{E}^a \cdot \boldsymbol{B}^a}\, d\tau'$$

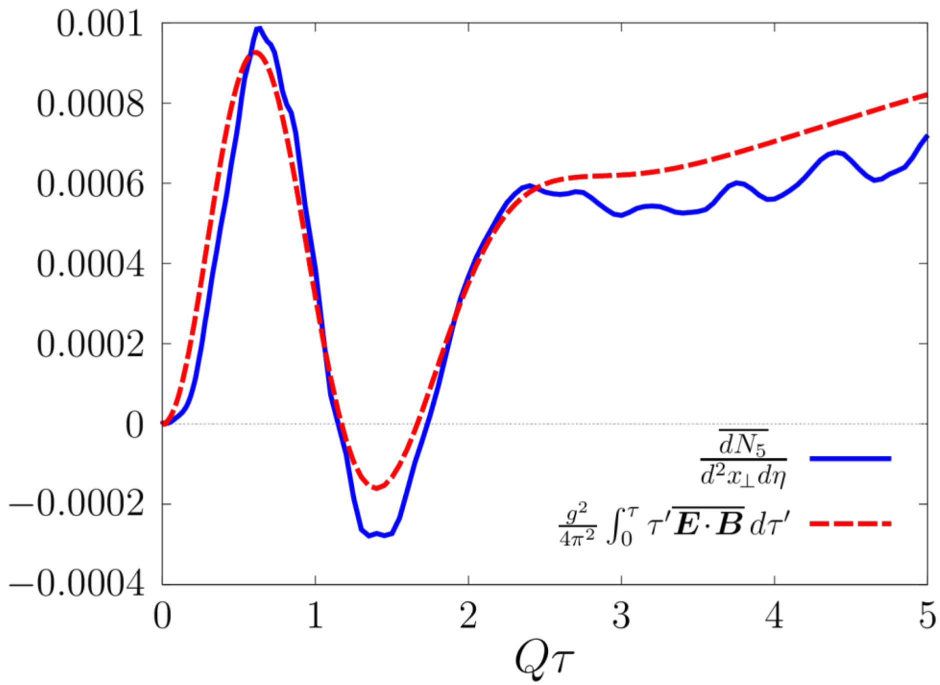

$m/Q = 0.01$

$N_x = N_y = 64,\ N_\eta = 256$

Glasma flux tubes

Verification of the space-averaged anomaly relation

$$\frac{\overline{dN_5}}{d^2x_\perp d\eta} \approx \frac{g^2}{4\pi^2}\int_0^\tau \tau' \overline{\boldsymbol{E}^a \cdot \boldsymbol{B}^a}\, d\tau'$$

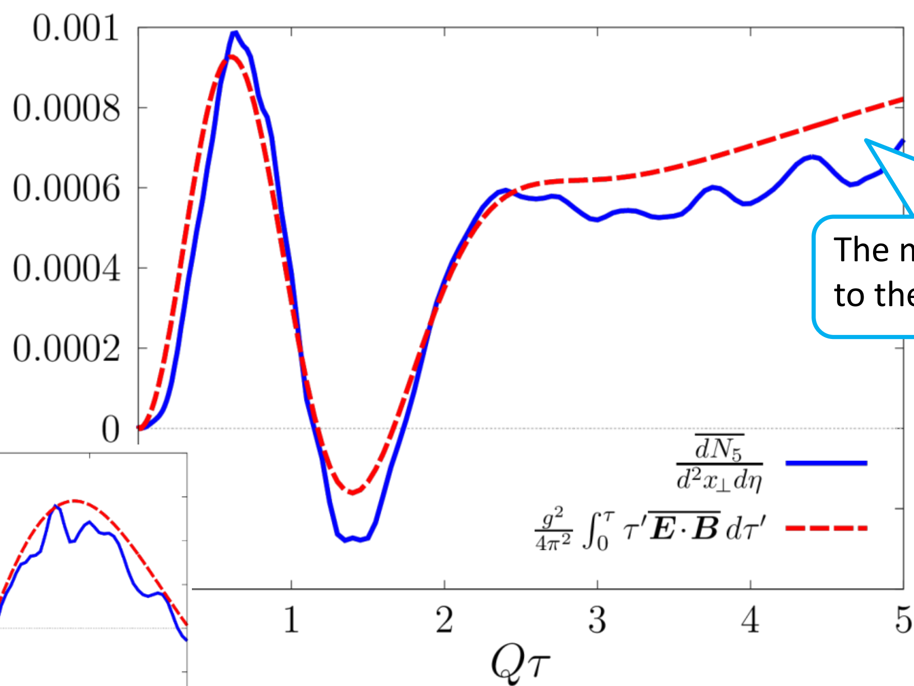

The monotonic increase corresponds to the decaying $\boldsymbol{E}\cdot\boldsymbol{B} \sim 1/\tau$.

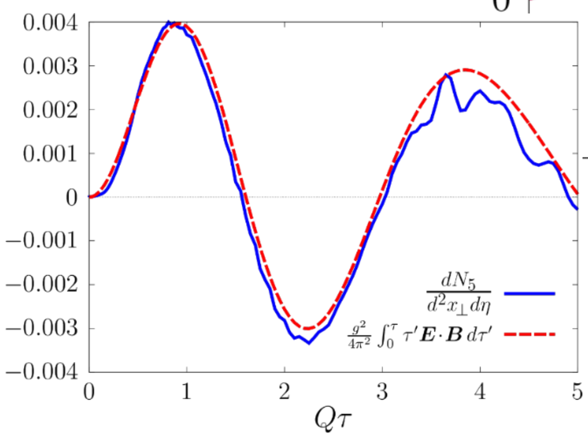

cf. Uniform case

$m/Q = 0.01$

$N_x = N_y = 64, \;\; N_\eta = 256$

Glasma flux tubes

Local anomaly budget

$$\frac{dN_5}{d^2x_\perp d\eta} + \int_0^\tau \tau' \partial_i j_5^i \, d\tau' \approx \frac{g^2}{4\pi^2} \int_0^\tau \tau' \boldsymbol{E}^a \cdot \boldsymbol{B}^a \, d\tau'$$

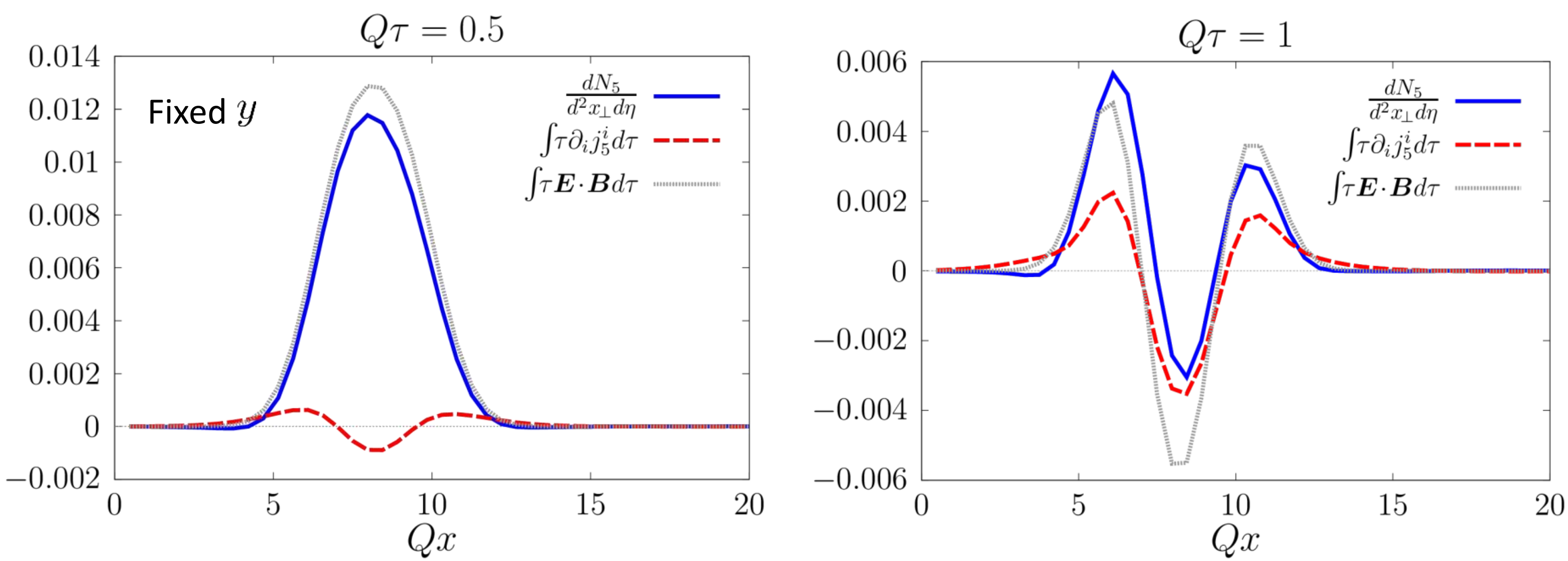

For $Q\tau \gtrsim 1$ the outflow term takes some fraction of the anomaly budget.

Summary and outlook

- The axial charge production in the longitudinally expanding geometry can be described by the real-time lattice simulations with the Wilson fermion.
- The classical gauge fields having nonzero $\boldsymbol{E}\cdot\boldsymbol{B}$ exhibit nontrivial behaviors.
- Because the axial charge density is related with the time integral of $\boldsymbol{E}\cdot\boldsymbol{B}$, it depends on the time history and it can remain even after $\boldsymbol{E}\cdot\boldsymbol{B}$ dies out.
- In inhomogeneous gauge fields, it is crucial to solve the Dirac equation for the proper description of the axial charge production including its spatial dynamics.

  - Real-time simulations of the Chiral Magnetic Effect in the expanding system by applying a U(1) magnetic field.
  - More realistic configurations?

Back up

Lattice formulation: Gauge sector

Gauge degrees of freedom: $U_i\,, U_\eta\,, E^i$ and $E^\eta \quad (i=1,2)$

Lattice Yang-Mills equations

$$\partial_\tau U_i(x) = ig\frac{a_\perp}{\tau}E^i(x)U_i(x)$$

$$\partial_\tau U_\eta(x) = iga_\eta \tau E^\eta(x)U_\eta(x)$$

$$\partial_\tau E^i(x) = -\frac{\tau}{ga_\perp^3}\sum_{j\neq i}\mathrm{Im}\left[U_{i,j}(x)+U_{i,-j}(x)\right]_{\mathrm{traceless}} - \frac{\tau}{g\tau a_\perp a_\eta^2}\mathrm{Im}\left[U_{i,\eta}(x)+U_{i,-\eta}(x)\right]_{\mathrm{traceless}}$$

$$\partial_\tau E^\eta(x) = -\frac{1}{g\tau a_\eta a_\perp^2}\sum_{i=1,2}\mathrm{Im}\left[U_{\eta,i}(x)+U_{\eta,-i}(x)\right]_{\mathrm{traceless}}$$

The clover definition for magnetic field is employed.

Lattice formulation: Quark sector

Dirac equation for the quark mode fucntions

$$\left(i\gamma^0\partial_\tau + \frac{i}{\tau}\gamma^3 D_\eta + i\gamma^i D_i - m + W\right)\psi^-_{\boldsymbol{p}_\perp,\nu,s,c} = 0$$

Tree-level improved lattice covariant derivative $c_1 = 4/3\,, c_2 = -1/6$

$$\begin{aligned}
D_\mu\psi(x) = \frac{c_1}{a_\mu}&\left[U_\mu(x)\psi(x+\hat{\mu}) - U^\dagger_\mu(x-\hat{\mu})\psi(x-\hat{\mu})\right] \\
&+ \frac{c_2}{a_\mu}\left[U_\mu(x)U_\mu(x+\hat{\mu})\psi(x+2\hat{\mu}) - U^\dagger_\mu(x-\hat{\mu})U^\dagger_\mu(x-2\hat{\mu})\psi(x-2\hat{\mu})\right]
\end{aligned}$$

Spatial Wilson term extended to the expanding geometry

$$\begin{aligned}
W\psi(x) = \frac{r_\perp}{2a_\perp}\sum_{i=1,2}&\left\{c_1\left[U_i(x)\psi(x+\hat{i}) - 2\psi(x) + U^\dagger_i(x-\hat{i})\psi(x-\hat{i})\right]\right. \\
&\left.+2c_2\left[U_i(x)U_i(x+\hat{i})\psi(x+2\hat{i}) - 2\psi(x) + U^\dagger_i(x-\hat{i})U^\dagger_i(x-2\hat{i})\psi(x-2\hat{i})\right]\right\} \\
&+ \frac{r_\eta}{2\tau a_\eta}\left\{c_1\left[U_\eta(x)\psi(x+\hat{\eta}) - 2\psi(x) + U^\dagger_\eta(x-\hat{\eta})\psi(x-\hat{\eta})\right]\right. \\
&\left.+2c_2\left[U_\eta(x)U_\eta(x+\hat{\eta})\psi(x+2\hat{\eta}) - 2\psi(x) + U^\dagger_\eta(x-\hat{\eta})U^\dagger_\eta(x-2\hat{\eta})\psi(x-2\hat{\eta})\right]\right\}
\end{aligned}$$